

# Experimental Study on the Thermal Shock Cracking of Cement Mortar

Tingting Wu

South China University of Technology

wu1355290727@163.com

**Abstract.** This paper explores the influence of heat shock on the cracking mode of cement mortar after experiencing different high temperatures (300 °C, 400 °C, 500 °C, 600 °C). Through the test, the paper reveals the crack law of cement mortar due to heat shock after experiencing different high temperatures, and the general relationship between different high temperatures and crack number, crack length, and crack width is analyzed and discussed. The test results show that the critical temperature of cement mortar cracking is 380 °C, and when the initial high temperature exceeds 500 °C, the crack pattern begins to appear hierarchical structure, and the characteristic performance of its hierarchy is more obvious with the increase of temperature. Moreover, the number of cracks, crack length and crack width gradually increase as the initial high-temperature increases.

**Keywords:** Temperature; Heat shock; Mortar; Crack

## 1. Introduction

With the development of the economy, concrete and high-strength mortar are also more and more widely used civil engineering structures, which then makes the study of its structural behavior after natural disasters become more and more important. Among many disasters, building structural fires may be the most common disaster and have become a social concern- -there are about 150,000 fires per year in China and about 3.6 million building structural fires per year worldwide [1-2]. Although they are widely considered in the construction industry as a kind of refractory when a fire occurs, materials such as concrete are exposed to high temperatures, their chemical composition, and physical properties will change seriously, and the mechanical properties of building materials and other affected seriously, make the loss of bearing capacity such as building components, even make building local or overall collapse and cause serious loss of life and property to human society.

In the event of a fire, the sprinkler is generally used to carry out fire rescue activities. This cooling method causes temperature mutation and heat shock. Because the concrete and mortar are thermal inert materials, the temperature gradient of the concrete produces under the action of thermal impact load, so that the interior of the object produces different expansion deformation. Due to the constraint effect of deformation coordination, it produces the constraint stress, that is, the instantaneous temperature stress from the surface and the interior of the building material. Cracks can occur when the temperature stress exceeds the tensile strength of the material. Research on thermal shock cracking earliest dates to the 1950s, Kingery [3] analysis material thermal stress due to thermal impact and puts forward the critical stress fracture based on thermal elastic stress analysis theory, Hasselman [4] based on fracture mechanics theory, from the perspective of energy, put forward the thermal shock resistance theory, analyze the material crack stroke and extension process under temperature change. Bahr [5-7] et others established a fracture mechanical model based on the variation of energy release rate in time to explain the thermal shock behavior. Bazant [8] and Nemat-Nasser [9] study the extension of cracks due to heat shock, and theoretically analyze and discuss the length hierarchy of cracks. In addition, many scholars [10-13] have also studied the phenomenon of thermal shock fracture expansion and fracture length hierarchy. After the thermal impact-related theory was put forward, scholars at home and abroad also carried out the thermal impact cracking experiment and numerical simulation research. In terms of ceramic materials, Shao [14-15] et al. studied the real crack mode of ceramic plates in the quenching state. Wu [16] and Jiang [17] et al. simulated the experimental results, which not only reproduced the crack evolution

in the process of heat shock but also found that the crack pattern has strict periodic and hierarchical characteristics; Ku [18] et al. used the crack length measurement method to reveal the influence of mechanical shock on ceramic heat shock in the quenching experiment. The results show that the compressive stress induced by mechanical impact produces fewer and shorter cracks on the ceramic samples in the water quenching experiment. In terms of concrete materials, Peng [19] studied the influence of thermal shock on the residual mechanical properties of fiber concrete. The test results show that, with the naturally cold

Table 1 Mix ratio of cement mortar

water-cement ratio	Cement/(Kg/m <sup>3</sup> )	sand/(Kg/m <sup>-3</sup> )	water/(Kg/m <sup>3</sup> )
0.55	417	1251	231

## 2. Methods

### 2.1 High-temperature test

An artificial intelligence box resistance furnace is used to treat the specimen at high temperatures to simulate the mortar in a high-temperature environment such as fire. The furnace size of the box resistance furnace is 60 cm 32 cm, as shown in Figure 1. Set the initial high-temperature T<sub>0</sub>, and the initial high temperature of each group of mortar specimens is set at 300°C, 400°C, 500°C and 600°C respectively. First, when the mortar specimen is heated up, take the heating rate of 10 C/min to the target temperature uniformly, and keep the constant temperature for 1.5 h. To avoid cracking in the heating process caused by excessive moisture in the mortar specimen, the mortar specimen must be dried in a 105 C drying box for 12 h before the high-temperature test.



Fig. 1 Box-type resistance furnace

Fig. 2 Heat shock test device diagram

### 2.2 Heat shock test

The cooling device is shown in Figure 2. A 90 cm 60 cm 25 cm square water tank is used, and two 150 mm pad blocks are placed in the water tank. Before the heat shock test, store 20 C water in the water tank in advance, and the initial water level is 1 cm lower than the pad height, to ensure the same initial water level before each test. The mortar specimen after high-temperature treatment is immediately removed and placed on the pad, and then the water level in the sink raises the water level to the lower surface of the contact mortar specimen so that the lower surface starts to cool down. This cooling process is maintained for 20 min. After the cooling ends, dry the specimen and describe the cracks on the observation surface with a red pen to observe the crack pattern formed by the mortar specimen during the heat shock process.

### 3. Test results and analysis

#### 3.1 The relationship between the crack mode and the number of cracks and the initial high-temperature T0 under heat shock

As shown in Figure 3, when T0 is 300°C, the surface color of the specimen is slightly red after cooling, and no cracks are observed. When T0 is 400°C, the surface color of the specimen deepens red after cooling than that of 300°C, causing large tensile stress on the lower surface, resulting in vertical sparse cracks on the lower surface of the specimen. When T0 is 500°C, the surface color of the specimen is slightly white after cooling, and the cracks begin to show the hierarchical structure of long and short cracks and the number of cracks increases. This is because the further expansion of the cleft in that critical state is unstable when a sufficiently large cooling penetration depth reaches the critical state. When the fracture expansion reaches the next stable critical state, some cracks stop expanding and gradually close, and some cracks increase with equal length with the continuous increase of the cooling penetration depth, so the crack pattern appears hierarchy [8]. When T0 is 600°C, the surface color of the specimen is deepened after cooling in white than that of 500°C, and the hierarchical structure of the long and short cracks is more obvious. At the same time, due to the inhomogeneity in the fine structure of the mortar material, the crack mode also shows an alternating expansion mode [23] disturbed by the unequal spacing of the cracks. By observing the different failure modes of the 4 groups of specimens, the crack mode of the mortar specimens evolves with the increase of the initial high-temperature T0 during the heat impact. The number of cracks at different initial high temperatures T0 is shown in Table 2, and the statistical results indicate that the number of specimen cracks increases with the increase of the initial high-temperature T0.

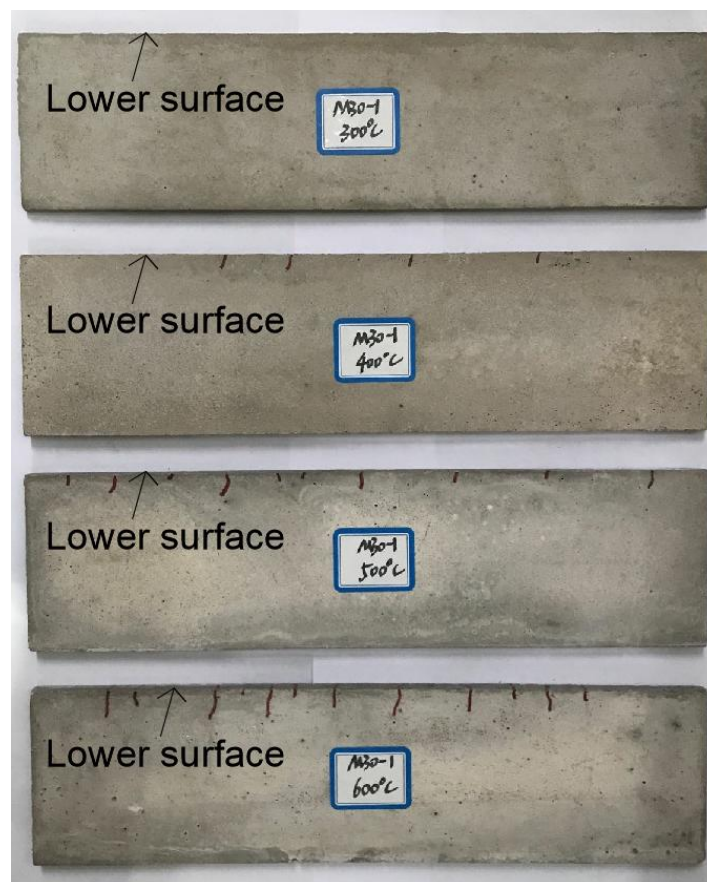


Figure 3 Heat shock crack patterns at different T0

Table 2. Number of cracks

number of cracks	$T_0=300^{\circ}\text{C}$	$T_0=400^{\circ}\text{C}$	$T_0=500^{\circ}\text{C}$	$T_0=600^{\circ}\text{C}$
M30-1	0	4	10	12
M30-2	0	4	11	11
M30-3	0	4	10	13
M30-4	0	7	10	12
M30-5	0	3	10	11
M30-6	0	3	11	13
average	0	4	10	12

### 3.2 Relationship between the crack length and the initial high-temperature $T_0$ under heat shock

The crack length of 6 pieces of mortar specimens was measured separately. The maximum crack length in all cracks in each group of specimens is counted  $l_{max}$  And the average of the length of all cracks in the observed surface of six specimens  $L$ . As shown in Figure 4 (a), M the 30 mortar specimen has no crack after heat shock of  $T_0$  of  $300^{\circ}\text{C}$  and  $l_{max}$  It is recorded as 0, mainly because the thermal stress caused by the temperature gradient between the temperature and  $20^{\circ}\text{C}$  water has not exceeded the tensile strength of the mortar specimen, so it cannot crack.  $T_0$  After the impact of  $400^{\circ}\text{C}$  heat, the mortar specimen begins to appear cracks, and the longest crack can reach up to 11.35mm, and the total length of the crack  $L$  is 32.11 mm. This is because the internal thermal stress of the specimen during cooling has reached the state of failure, which leads to the occurrence of cracks. Therefore, the critical temperature gradient of the mortar specimen cracking is  $380^{\circ}\text{C}$ .  $T_0$  After the heat impact of  $500^{\circ}\text{C}$ , the longest crack can reach 13.69 mm, which increased by 20.62% compared with  $400^{\circ}\text{C}$ , and the total length  $L$  increased by 151.45% compared to  $400^{\circ}\text{C}$ . along with  $T_0$ . As the temperature gradient of the lower surface of the specimen increases, as the cooling continues, the low-temperature area extends to the inside of the sample. Thus, the tensile stress at the fracture tip increases further, driving the fracture to continue to expand, resulting in an increased maximum fracture length and the mean total fracture length. The crack pattern of long and short cracks after  $T_0$  of  $600^{\circ}\text{C}$  heat shock is more obvious,  $l_{max}$  Up to 18.43 mm, compared to  $500^{\circ}\text{C}$ ,  $l_{max}$  Increased by 34.62% and  $L$  by 47.1%. With the increase of  $T_0$ , there is a larger temperature gradient on the lower surface of the mortar test during cooling. The temperature gradient on the lower surface increases from  $380^{\circ}\text{C}$  to  $580^{\circ}\text{C}$ . The temperature of water further reduces the temperature on the lower surface and leads to the tensile stress concentration near the crack tip, which drives the crack to expand steadily as the cooling front penetrates deeper into the specimen until the temperature gradient can no longer produce enough concentrated stress to drive the crack expansion. According to the results, the total crack length  $L$  and the maximum crack length of the mortar specimen after cooling  $l_{max}$  All increase with the initial high temperature  $T_0$ .

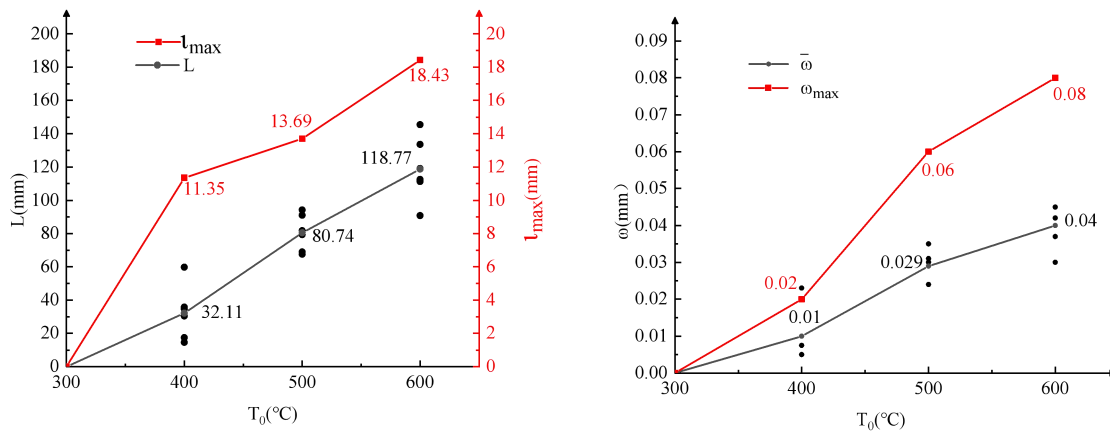


Figure 4 Change curve of crack length and crack width at different  $T_0$ : (a) crack length, (b) crack width

### 3.3 Relationship between crack width and initial high-temperature $T_0$ under heat shock

The crack width meter is used to measure the crack width of 6 mortar specimens. In this experiment, the width of each crack on the specimen surface is measured at 3 mm from the lower surface end of the specimen. All crack widths of each specimen were averaged to observe the change of crack width with the initial high temperature of heat shock, and to obtain the maximum crack width after heat shock  $w_{max}$  and the average crack width  $\bar{w}$ . As shown in Figure 4 (b). When  $T_0$  is 300°C, the crack width is 0. When the  $T_0$  is 400°C  $w_{max}$  up to 0.02 mm,  $\bar{w}$  is at 0.01 mm. Maximum crack width after the initial temperature  $T_0$  exceeds 400°C  $w_{max}$  and the average crack width  $\bar{w}$ . The overall trend presents a gradually increasing trend.  $T_0$  at 500°C  $w_{max}$  increased 0.04 mm more than 400 °C,  $\bar{w}$  increased by 0.019 mm.  $T_0$  for the 600°C of the same time  $w_{max}$  up by 33.33% from 500°C,  $\bar{w}$  that increased by 37.93 percent. It can be seen that the crack width of the mortar specimen increases gradually with the increase of the initial high temperature. When the initial high temperatures  $T_0$  rise, cooling the increase of the temperature gradient is not only driving crack expansion to crack length increase, but also makes the crack width increase, but  $T_0$  is 500°C heat impact after the average crack length  $L$  growth rate compared to the average crack width fast, shows that  $T_0$  for 500°C after the crack expansion along the length direction of the width direction is obvious.

## Conclusion

Through heat shock test of four groups of M30 mortar materials at different initial high temperatures, obtaining different crack patterns after heat shock of mortar specimens, and analyzing the influence of different initial high temperatures on the number of cracks, crack length, and crack width. The following conclusions can be obtained:

The number of cracks increased with the initial high temperature. The mortar specimen began to crack after the initial high temperature of 400°C heat shock. The cracks of the mortar specimen after the initial high temperature of 500°C heat impact begin to show the hierarchical structure of long and short cracks, and the hierarchical structure of the cracks is more obvious with the increase of the initial high temperature.

The critical temperature gradient of thermal shock cracking of the M30 mortar specimen is 380°C. The higher the initial high temperature at the heat shock, the higher the crack length.

The maximum and mean crack width increase with the initial high temperature during heat shock.

## References

- [1] WU B, TANG G. State-of-the-art of fire-resistance study on concrete structures in recent years [J]. *Jianzhu Jiegou Xuebao/Journal of Building Structures*, 2010, 31(6): 110-21.
- [2] ZHENG W, HOU X, WANG Y. Progress and the prospect of fire resistance of reinforced concrete and prestressed concrete structures [J]. *Harbin Gongye Daxue Xuebao/Journal of Harbin Institute of Technology*, 2016, 48(12): 1-18.
- [3] KINGERY W D. Factors Affecting Thermal Stress Resistance of Ceramic Materials [J]. *Journal of the American Ceramic Society*, 1955, 38(1): 3-15.
- [4] HASSELMAN D P H. Griffith criterion and thermal shock resistance of single-phase versus multiphase brittle ceramics [J]. *Journal of the American Ceramic Society*, 1969, 52(5): 288-9.
- [5] BAHR H A, FISCHER G, WEISS H J. Thermal-shock crack patterns explained by single and multiple crack propagation [J]. *Journal of Materials Science*, 1986, 21(8): 2716-20.
- [6] BAHR H A, BALKE H, KUNA M, et al. Fracture analysis of a single edge cracked strip under thermal shock [J]. *Theoretical and Applied Fracture Mechanics*, 1987, 8(1): 33-9.
- [7] BAHR H A, WEISS H J, MASCHKE H G, et al. Multiple crack propagation in strip caused by thermal shock [J]. *Theoretical and Applied Fracture Mechanics*, 1988, 10(3): 219-26.
- [8] BAZANT Z P, OHTSUBO H, AOH K. Stability and post-critical growth of a system of cooling or shrinkage cracks [J]. *International Journal of Fracture*, 1979, 15(5): 443-56.
- [9] KEER L M, NEMAT-NASSER S, ORANRATNACHAI A. Unstable growth of thermally induced interacting cracks in brittle solids: further results [J]. *International Journal of Solids and Structures*, 1979, 15(2): 111-26.
- [10] COLLIN M, ROWCLIFFE D. The morphology of thermal cracks in brittle materials [J]. *Journal of the European Ceramic Society*, 2002, 22(4): 435-45.
- [11] GUPTA T K. Strength degradation and crack propagation in thermally shocked Al<sub>2</sub>O<sub>3</sub> [J]. *Journal of the American Ceramic Society*, 1972, 55(5): 249-53.
- [12] TANG S B, ZHANG H, TANG C A, et al. Numerical model for the cracking behavior of heterogeneous brittle solids subjected to thermal shock [J]. *International Journal of Solids and Structures*, 2016, 80: 520-31.
- [13] HASSELMAN D P H. On the nature of crack propagation during thermal shock of brittle ceramics [M]. 1996.
- [14] SHAO Y F, SONG F, LIU B Y, et al. Observation of ceramic cracking during quenching [J]. *Journal of the American Ceramic Society*, 2017, 100(2): 520-3.
- [15] SHAO Y F, XU X H, MENG S H, et al. Crack Patterns in Ceramic Plates after Quenching [J]. *Journal of the American ceramic society*, 2010, 93(10): 3006-8.
- [16] WU X F, JIANG C P, SONG F, et al. Size effect of thermal shock crack patterns in ceramics and numerical predictions [J]. *Journal of the European ceramic society*, 2015, 35(4): 1263-71.
- [17] JIANG C P, WU X F, LI J, et al. A study of the mechanism of formation and numerical simulations of crack patterns in ceramics subjected to thermal shock [J]. *ACTA MATERIALIA*, 2012, 60(11): 4540-50.
- [18] KOU H, LI W, ZHANG X, et al. Effects of mechanical shock on thermal shock behavior of ceramics in quenching experiments [J]. *Ceramics International*, 2017, 43(1): 1584-7.
- [19] PENG G-F, BIAN S-H, GUO Z-Q, et al. Effect of thermal shock due to rapid cooling on residual mechanical properties of fiber concrete exposed to high temperatures [J]. *Construction and Building Materials*, 2008, 22(5): 948-55.
- [20] NASSIF A Y. Postfiring stress-strain hysteresis of concrete subjected to various heating and cooling regimes [J]. *Fire and materials*, 2002, 26(3): 103-9.
- [21] CHENG J, CHANG X L, LI T C. Temperature Induced Cracking Analysis for Lushui Pier Using LFM [Z]. *Advance in Industrial and Civil Engineering*, PTS 1-4. 2012: 1913-6.10.4028/www.scientific.net/AMR.594-597.1913

- [22] ANTONOVICH V, ZDANEVICIUS P, STONIS R, et al. Study on the Destruction of Heat-Resistant Chamotte Concrete During Sharp Heating and Cooling [J]. Refractories and industrial ceramics, 2020, 61(3): 326-31.
- [23] BAHR H A, BAHR U, PETZOLD A. 1-deterministic crack pattern formation as a growth process with restrictions [J]. Europhysics Letters, 1992, 19(6): 485-90.